PETROGENESIS OF AND SUBSOLIDUS REEQUILIBRATION WITHIN LUNAR FERROAN ANORTHOSITES: TWO DEMONSTRATIONS OF A NEW fO_2-DEPENDENT MODEL FOR PLAGIOCLASE-MELT EUROPIUM PARTITIONING. N. Dygert[1], D. Ji[1], A.L. Fagan[2], C.R. Neal[3], D.S. Draper[4], J.F. Rapp[5], T.J. Lapen[6]. [1]Department of Earth and Planetary Sciences, University of Tennessee, Knoxville, TN, 37916, (ndygert1@utk.edu), [2]Western Carolina University, Cullowhee, NC, [3]University of Notre Dame, Notre Dame, IN, [4]NASA Headquarters, Washington D.C., [5]NASA Johnson Space Center, Houston, TX, [6]University of Houston, Houston, TX.

Introduction: Partitioning of the multivalent element Eu between plagioclase and coexisting silicate melt is known to depend on oxygen fugacity (fO_2) [e.g., 1]. This is a consequence of Eu exhibiting 3+ valence under oxidizing conditions and 2+ valence under reducing conditions, as well as the dramatically differing partitioning behavior of trivalent and divalent Eu in plagioclase, the former being highly incompatible and the latter being compatible (~D_{Sr}) [e.g., 1, 2]. Using new experimental observations and literature data, Dygert et al. [3] parameterized a predictive model for the partitioning of Eu between plagioclase and silicate melt as a function of fO_2 [e.g., 1,4]:

$$D_{Eu} = \frac{K \cdot D_{Eu^{2+}} + D_{Eu^{3+}} \cdot (fO_2)^{\frac{1}{4}}}{K + (fO_2)^{\frac{1}{4}}}, \quad (1)$$

where K is a constant ($9.46\times10^{-4} \pm 5.5\times10^{-4}$) and $D_{Eu^{2+}}$ and $D_{Eu^{3+}}$ are T and An# dependent plagioclase-melt partition coefficients for divalent and trivalent Eu predicted from [5]. Within a factor of 2, Eq. 1 reproduces experimental observations over >15 orders of magnitude variation in fO_2 in lunar and terrestrial compositional systems ranging from basalts to dacites. This model can be rearranged as a Eu-in-plagioclase-melt oxybarometer:

$$log(fO_2) = -4 \times log\left(\frac{D_{Eu}^{2+} - D_{Eu}}{K \cdot (D_{Eu} - D_{Eu}^{2+})}\right). \quad (2)$$

Applied to experimentally rehomogenized plagioclase-hosted melt inclusions from mid-ocean ridge basalts (MORBs) [6], Eq. 2 recovers fO_2s (~FMQ) consistent with independent methods [e.g., 7], demonstrating the applicability of Eqs. 1 & 2 to natural systems. The supplement to [3] includes a downloadable spreadsheet that can be used to calculate D_{Eu} as a function of plagioclase composition, T, and fO_2, and a plagioclase-melt oxybarometer that can be applied to calculate fO_2 from measured Eu distributions in well equilibrated plagiolase-melt pairs.

Model Predictions: Fig. 1a shows D_{Eu} predicted using Eq. 1 as a function of fO_2 and plagioclase An#. For lunar-relevant An#s (~90), D_{Eu} is predicted to change by more than two orders of magnitude across the range of possible fO_2 conditions; D_{Eu} is ~1 at the lunar-relevant iron-wüstite buffer (IW). Fig. 1b shows Eu and REE partition coefficients predicted as a function of T and fO_2. Note that D_{Eu} exhibits relatively little T sensitivity at low, lunar-relevant fO_2s, but becomes more temperature sensitive under oxidizing conditions. Because trivalent REE partition coefficients decrease with decreasing temperature [e.g., 5], the magnitude of the D_{Eu} anomaly increases as temperature decreases.

Eu anomalies in plagioclase after lunar magma ocean (LMO) solidification: Important evidence for an LMO comes from positive Eu anomalies in lunar anorthites (Eu/Eu*, where Eu*=$\sqrt{Sm \times Gd}$, chondrite normalized), and corresponding negative anomalies in rocks thought to originate from sources from the LMO complementary to the crust (e.g., basalts). Using Eq. 1 and models for lunar magma ocean solidification, Eu partitioning can be predicted and the distribution of Eu in natural samples can be compared to models to provide new insights into the formation and subsequent evolution of the anorthositic cumulate flotation crust. Here we calculated REE abundances in plagioclase that fractionated from the LMO as a function of fO_2, according to the experiments of [8], assuming a bulk Moon with terrestrial

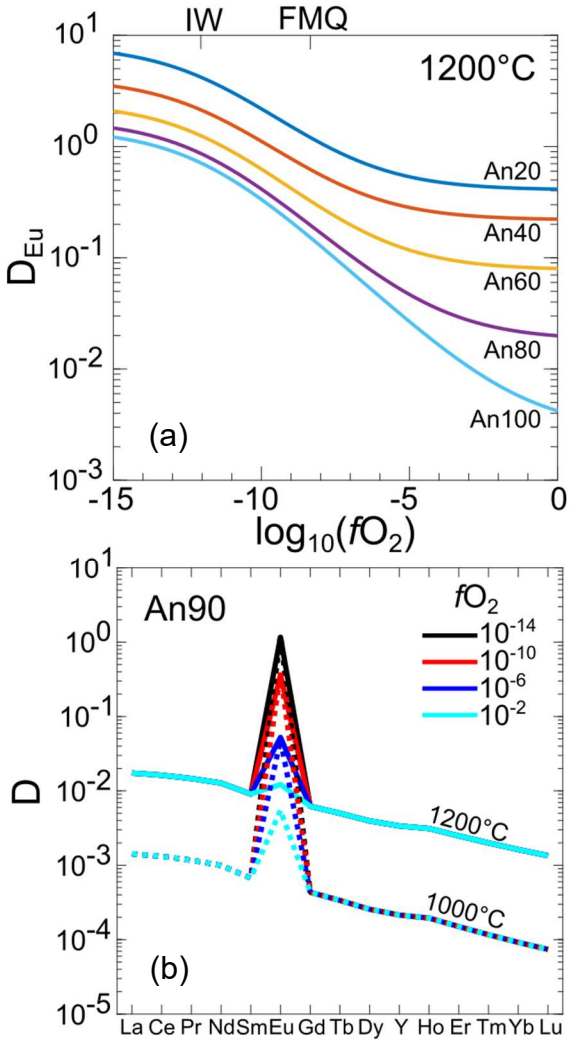

Fig. 1. Eu partition coefficients predicted as a function of fO_2 and An# at a T of 1200°C **(a)**. Note the especially strong dependence of D_{Eu} on fO_2 at lunar-relevant An#s. Eu and REE partition coefficients predicted as a function of T and fO_2 at a An90 **(b)** [3,5]. The figure highlights the importance of T as well as fO_2 in determining the Eu partitioning anomaly.

N-MORB trace element abundances [9, 10] (Fig. 2). To first order, simulations assuming chondritic and depleted MORB mantle (DMM) sources produce similar elemental distributions (at slightly different Ce/Sm ratios, not shown). The simulation results suggest that LMO solidification alone cannot reproduce the compositions of the ferroan anorthosites. Subsequent processing in the form of subsolidus reequilibration during cooling and/or the addition of a KREEP component can reproduce the compositions, as indicated schematically by the arrows in Fig. 2. Addition of a KREEP component may have been achieved in a Serial Magmatism-type scenario [e.g., 12].

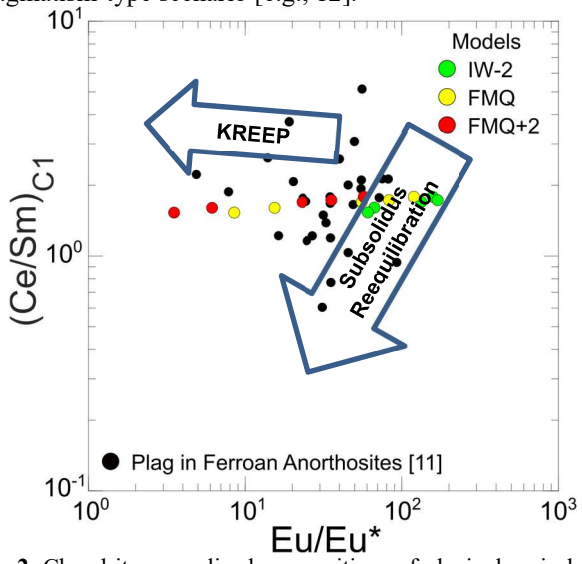

Fig. 2. Chondrite normalized compositions of plagioclase in lunar anorthosites (colored circles) calculated using a LMO solidification model for a range of fO_2s (Eq 1., [5]) assuming fractional crystallization of a bulk Moon with N-MORB trace element abundances [8,9]. Black circles are plagioclase in returned ferroan anorthosites [11]. For lunar relevant fO_2s, only a small fraction of the data can be explained by fractionation from an LMO alone. Subsolidus reequilibration and/or KREEP assimilation may be invoked to explain the distribution of the natural samples.

Formation of a ferroan anorthosite with positive and negative Eu/Eu*: Lunar impact melt rock 60635,2 contains plagioclase that are unzoned in major elements but exhibit positive Eu anomalies associated with REE enrichment and negative Eu anomalies associated with relative REE depletion, at the thin section scale [Fig. 3, e.g., 13]. We evaluated two possibilities for formation of the Eu and trace element distributions under variable fO_2 conditions [3]. (1) Fractional crystallization of an initially Eu-enriched melt, which would eventually produce a Eu depleted, Ce-enriched plagioclase as it crystallized (Fig. 3a), and (2), redistribution of Eu after subsolidus heating in an oxidizing environment, perhaps after impact bombardment (Fig. 3b).

Fig. 3a shows that Eu/Eu* and Ce abundances cannot both be satisfied in fractional crystallization scenarios, regardless of fO_2. The slope of the fractionation trends are too steep in Ce vs. Eu/Eu* space. In contrast, subsolidus exchange between plagioclase and coexisting pyroxenes under increasing fO_2 conditions during heating matches the curvature and distribution of the data well (Fig 3b). Increasing oxidation state with T may be attributed to the fact that oxygen activity increases with T for a buffered assemblage, and perhaps suggest addition of an oxidized component from an impactor.

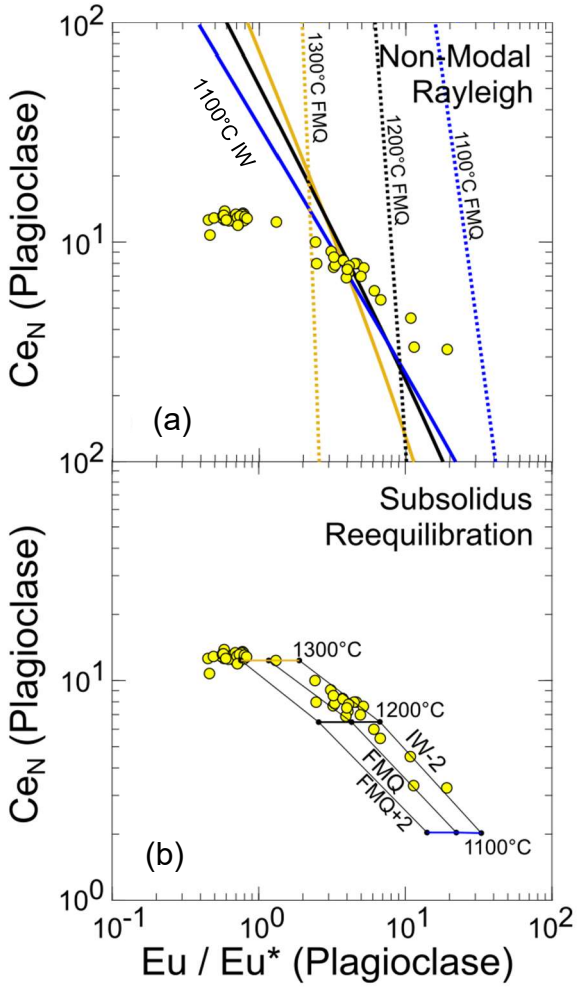

Fig. 3. Chondrite normalized Ce vs. Eu/Eu* in 60635,2 plagioclase (yellow circles), compared to non-modal fractional crystallization models **(a)** (solid and dotted colored lines, IW and FMQ, respectively), and models for subsolidus reequilibration as a function of fO_2 and T, **(b)**, indicated by the grid. The curvature of the subsolidus reequilibration models better fits the data.

References: [1] Drake (1975) *GCA* **39**, 55-64. [2] Bindeman et al. (1998) *GCA* **62**, 1175-1193. [3] Dygert, et al. (2020) *GCA* **279**, 258-280. [4] Wilke & Behrens (1999) *CMP* **137**, 102-114. [5] Sun et al. (2017) *GCA* **206**, 273-295. [6] Nielsen et al. (2017) *G*^{3}. [7] Cottrell & Kelley (2011) *EPSL* **305**, 270-282. [8] Rapp & Draper (2018) *MAPS* **53**, 1452-1455. [9] Arevalo & McDonough, *Chem. Geol.* **271**, 70-85. [10] Boyet & Carlson (2007) *EPSL* **262**, 505-516. [11] Pernet-Fisher et al. (2019) *GCA* **266**, 109-130. [12] Longhi (2003) *JGR* **108**, E8, 5083. [13] Fagan & Neal (2012) *LPSC* **43**, #1426 (abstr.).